ANNALS of Clinical and Translational Neurology
Open Access
ANA American Neurological Association

RESEARCH ARTICLE

A novel dysferlin mutant pseudoexon bypassed with antisense oligonucleotides

Janice A. Dominov[1], Özgün Uyan[1], Peter C. Sapp[1], Diane McKenna-Yasek[1], Babi R. R. Nallamilli[2], Madhuri Hegde[2] & Robert H. Brown Jr.[1]

[1]Neurology Department, University of Massachusetts Medical School, Worcester, Massachusetts, 01605
[2]Department of Human Genetics, Emory University School of Medicine, Atlanta, Georgia, 30322

Correspondence
Robert H. Brown Jr, Neurology Department, S5-755, University of Massachusetts Medical School, 55 Lake Avenue North, Worcester, MA 01655. Tel: (508) 334-1271; Fax: (508) 856-6778; E-mail: Robert.Brown@umassmed.edu

Funding Information
We thank the Cecil B. Day Foundation for supporting this work. R. H. B.'s laboratory also receives support from the NINDS (R01 FD004127-02, 5 R01 NS079836-03, 5 R01 NS065847-05, 1 R01 NS073873-03). P. C. S. is funded through the auspices of Dr. H. Robert Horvitz, an Investigator of the Howard Hughes Medical Institute (Massachusetts Institute of Technology). We also thank the Jain Foundation for providing support for M. H.

Received: 24 July 2014; Revised: 1 August 2014; Accepted: 4 August 2014

***Annals of Clinical and Translational Neurology* 2014; 1(9): 703–720**

doi: 10.1002/acn3.96

Abstract

Objective: Mutations in dysferlin (DYSF), a Ca^{2+}-sensitive ferlin family protein important for membrane repair, vesicle trafficking, and T-tubule function, cause Miyoshi myopathy, limb-girdle muscular dystrophy type 2B, and distal myopathy. More than 330 pathogenic *DYSF* mutations have been identified within exons or near exon–intron junctions. In ~17% of patients who lack normal DYSF, only a single disease-causing mutation has been identified. We studied one family with one known mutant allele to identify both the second underlying genetic defect and potential therapeutic approaches. **Methods**: We sequenced the full *DYSF* cDNA and investigated antisense oligonucleotides (AONs) as a tool to modify splicing of the mRNA transcripts in order to process out mutant sequences. **Results**: We identified a novel pseudoexon between exons 44 and 45, (pseudoexon 44.1, PE44.1), which inserts an additional 177 nucleotides into the mRNA and 59 amino acids within the conserved C2F domain of the DYSF protein. Two unrelated dysferlinopathy patients were also found to carry this mutation. Using AONs targeting PE44.1, we blocked the abnormal splicing event, yielding normal, full-length *DYSF* mRNA, and increased DYSF protein expression. **Interpretation**: This is the first report of a deep intronic mutation in *DYSF* that alters mRNA splicing to include a mutant peptide fragment within a key *DYSF* domain. We report that AON-mediated exon-skipping restores production of normal, full-length *DYSF* in patients' cells in vitro, offering hope that this approach will be therapeutic in this genetic context, and providing a foundation for AON therapeutics targeting other pathogenic *DYSF* alleles.

Introduction

Dysferlin (DYSF) is a member of the ferlin family of Ca^{2+}-dependent phospholipid-binding proteins that functions in membrane vesicle fusion, membrane repair, T-tubule stability, and Ca^{2+} homeostasis.[1,2] Insufficient DYSF leads to muscular dystrophies (dysferlinopathies) that include Miyoshi myopathy (MM), limb-girdle muscular dystrophy type 2B (LGMD-2B), and distal myopathy with anterior tibial onset (DMAT).[3,4] These recessively inherited diseases are characterized by muscle weakness beginning in late teens to early twenties. Clinical symptoms include progressive, largely symmetrical weakness, and elevated serum creatine kinase (CK) indicative of muscle damage, inflammation, and abnormal muscle morphology.[5–8] As with other forms of muscular dystrophy, there is currently no primary treatment for dysferlinopathies; there is a compelling need for new therapeutic approaches to treat these diseases.

As a member of the ferlin family, DYSF has seven Ca^{2+}-sensitive phospholipid binding C2 domains (C2A through C2G) that vary in their phospholipid binding characteristics,[9] relative importance for DYSF dimerization[10] and membrane interaction,[11] and collectively may alter the structure of lipid bilayers, facilitating membrane fusion and interaction with other proteins.[12] DYSF interacts with a number of proteins that function in membrane trafficking and fusion including caveolin-3,[13]

annexins A1 and A2,[14] affixin,[15] calpain-3,[16] MG53[17], and AHNAK.[18] Through these interactions, DYSF plays an important role in sarcolemma repair following membrane damage as well as vesicle trafficking, membrane turnover,[5,19] and T-tubule formation and function.[20–22]

DYSF (237 kDa) is derived from a ~6.2 kb transcript assembled from up to 55 exons. There are 14 isoforms of *DYSF* that arise from use of two separate promoters and alternate exon splicing, with isoform 8 being predominant in skeletal muscle.[23] Disease-causing mutations in *DYSF* occur throughout the gene with no obvious hot spots or correlations with specific disease features.[24] Genetic data compiled in Universal Mutation Database for Dysferlin (UMD-DYSF, v.1.1 26 April 2013, http://www.umd.be/DYSF/)[24] list 337 disease-causing mutations that have been found in 725 patients worldwide. Approximately 48% of these patients are homozygous for specific mutations, while the remaining 52% are heterozygous and ~17% of patients have only one pathogenic mutant allele identified through standard exon sequencing approaches used to screen for mutations. The unknown mutations in other pathogenic alleles likely reside within intronic or regulatory regions not typically interrogated in such assays. Alternative approaches are required to identify these other mutant alleles.

We have studied two such heterozygous MM patients (siblings) for whom only one pathogenic mutant allele has been defined despite multiple sequencing efforts examining *DYSF* exons and flanking intronic regions. These patients lack normal DYSF in their muscles and are heterozygous for a nonsense mutation in exon 32. To identify the second unknown mutation, we looked directly for alterations in the mRNA expressed in myogenic cells from these patients. We identified a deep intronic point mutation within intron 44 (44i) that leads to abnormal mRNA and protein structure. In addition, we report partial restoration of normal *DYSF* mRNA and DYSF protein levels in myogenic cells from these patients using antisense oligonucleotides (AONs) to bypass the pseudoexon created by the 44i mutation, providing a novel therapeutic approach to restore *DYSF* function.

Materials and Methods

Patients

Two MM patients (ID# 8597, 8601, designated herein as P1 and P2, respectively) are siblings that exhibited typical MM disease symptom onset and progression. In their early twenties, they developed difficulty walking on their toes and myalgias, and were found to have very elevated serum CK levels (more than 100-fold elevated). Subsequently, they developed progressive distal to proximal leg weakness and atrophy, followed in their late thirties and early forties with some hand weakness. Muscle biopsies performed in the initial stages of the disease revealed muscle degeneration with fatty replacement. After the discovery of DYSF in 1998, a repeat muscle biopsy was performed in the older brother; no DYSF was detected by immunostaining or immunoblotting in that specimen. Analogously, little or no DYSF was detectable in monocytes from either brother. Exon sequencing determined that they are heterozygous for a nonsense mutation in *DYSF* exon 32 (c.3444_3445delTGinsAA, p.Y1148X) that causes a premature stop codon within the C2D domain. Further sequencing analyses failed to identify a second pathogenic allele, suggesting that this mutation lies within noncoding regions of the gene. Skin biopsies and blood were collected from these patients and their immediate relatives to generate dermal fibroblast cell cultures and for DNA analyses. The fibroblasts were used to develop myogenic cell culture lines.

In the initial phase of this study, we screened DNAs from 114 patients with a clinical diagnosis of MM, representing 81 pedigrees. Included in this set was the index family, patients P1 and P2. In a second phase of the study, we were provided DNA samples from eight unrelated MM individuals who were DYSF negative in monocyte assays and for whom at least one of the pathogenic *DYSF* mutations had not been identified by exon sequencing (some of which previously described[25]). DNAs from an additional 724 individuals without muscle disease (either clinically normal or with unrelated conditions) were used in these studies. Patient materials were collected after informed consent was obtained and all protocols were approved by the University of Massachusetts Medical School or Emory University School of Medicine Institutional Review Boards.

Cell cultures

Dermal fibroblast cultures

Patient skin biopsies were obtained under the auspices of an Institutional Review Board-approved protocol with informed consent and cultured as explants in Roswell Park Memorial Institute (RPMI) Medium (RPMI1640 [Gibco, Grand Island, NY, USA]) or Dulbecco's Modified Eagle Medium (DMEM Glutamax with pyruvate [Gibco]), each containing 15% fetal bovine serum (FBS) (Sigma, St. Louis, MO, USA), 100 units/mL penicillin, 100 μg/mL streptomycin, and 0.25 μg/mL Fungizone [Gibco]) to generate fibroblast lines. These were later routinely passaged in DMEM Fibroblast Growth Medium (GM) (DMEM, 15% FBS, 1× Non-Essential Amino Acids [Gibco], 10 mmol/L HEPES (N-2-hydroxyethylpiperazine-N-2-ethane sulfonic acid) [Gibco]). We also obtained normal adult human dermal fibroblasts from American Type Culture Collection (ATCC, Manassas, VA, USA) (termed NHDF-2).

Myogenic conversion of dermal fibroblasts and myoblast lines

We established inducible fibroblast-derived myogenic (iFDM) cell cultures from patient and normal NHDF fibroblast lines using methods described.[26,27] Fibroblasts were transduced with a tamoxifen-inducible MyoD lentivirus (Lv-CMV-MyoD-ER(T),[26] Addgene, Cambridge, MA, USA). These cells proliferate as fibroblasts until induced to express MyoD by 4-hydroxytamoxifen (TMX) treatment (5 μmol/L TMX [Sigma, H-7904]) in GM for 1 day followed by 3 days in 1 μmol/L TMX in differentiation medium (DM) (DMEM Glutamax with pyruvate: Medium 199 [Gibco] (3:1), 2% horse serum [HyClone, Logan, UT, USA], 20 mmol/L HEPES, and 20 μg/mL insulin, 11 μg/mL transferrin, 1.3 μg/mL selenium [2× ITS, Gibco]), replacing DM every third day. In initial experiments, TMX was added throughout the differentiation period, but equivalent differentiation was observed with 3 days of treatment, so the TMX induction in DM was shortened to 3 days. Some fibroblasts were also immortalized by transduction with an hTERT lentiviral vector (Lv-CMV-hTERT-IRES-Puro, UCLA Vector Core,[27]) prior to myogenic conversion with the MyoD lentivirus, extending the proliferative potential of these cells.

We also obtained a myoblast cell line (01Ubic-CT2 ["UBic"]) (Dr. Charles Emerson, UMass Medical School Wellstone Muscular Dystrophy Cooperative Research Center) derived from normal human biceps muscle and immortalized by transduction with hTERT and CDK4 retroviruses[28] to generate an unrestricted supply of "normal" myogenic cells.

Immunocytochemistry

Differentiated iFDM cells were fixed with 4% paraformaldehyde for 10 min then permeabilized and immunostained using antimyosin heavy chain antibody (MF20, monoclonal supernatant 1/10 dilution, Developmental Studies Hybridoma Bank, U. of Iowa) and detected with Alexa 488 anti-mouse IgG (Invitrogen, Grand Island, NY, USA) and Hoechst 33258 to stain nuclei with methods as described.[29]

Protein analysis

Proteins were extracted from differentiated iFDM cells using Radio-Immunoprecipitation Assay (RIPA) buffer (40 mmol/L Tris–HCl pH 8, 150 mmol/L sodium chloride 1% Triton X-100, 0.5% sodium deoxycholate, 0.5% SDS) with protease inhibitors (complete, Roche, Indianapolis, IN, USA) then a sample was quantified using a BCA (bicinchoninic acid) protein assay (Thermo Fisher Scientific, Waltham, MA, USA). The remaining protein was heated at 70°C in sodium dodecyl sulfate polyacrylamide gel electrophoresis (SDS-PAGE) Laemmli sample buffer 10 min then separated on 7.5% acrylamide TGX SDS–PAGE gels (Bio-Rad, Hercules, CA, USA), blotted onto nitrocellulose filters using an iBlot Gel Transfer Device (Life Technologies, Grand Island, NY, USA, program P3, 10 min), and analyzed by western immunostaining using LI-COR Odyssey blocking reagent and methods as described.[30] Primary antibodies included and anti-DYSF specific for the C-terminal end (NCL-Hamlet, Leica Biosystems, Buffalo Grove, IL, USA, 1/1000) or N-terminal end (Romeo, JAI-1-49-3, Abcam, Cambridge, MA, USA, 1/500), and anti-glyceraldehyde-3-phosphate dehydrogenase (GAPDH) (10R-G109a Fitzgerald, Acton, MA, USA, 1/1000). Blots were quantitatively analyzed using a LI-COR Odyssey infrared imager.

Nucleic acid purification and reverse transcription

Genomic DNA and RNA were prepared from cells using Gentra Puregene (Qiagen, Valencia, CA, USA) and TRIzol (Life Technologies) reagents, respectively, following manufacturer's protocols. RNA was DNAse digested (TURBO DNA-Free, Ambion, Austin TX, USA), to remove DNA contaminants then 0.2–2 μg RNA was reverse transcribed (High Capacity cDNA Reverse Transcription Kit; Applied Biosystems, Foster City, CA, USA) using manufacturer's protocols.

PCR amplification

For all RNA and cDNA analyses, we used *DYSF* mRNA variant 8 (NM_003494.3) as the reference sequence, as it is the predominant isoform in skeletal muscle. We first used polymerase chain reaction (PCR) primers to amplify and sequence the cDNA from patient and normal iFDM cells to determine whether the exon 32 (c.3444_3445delTGinsAA) mutant allele is expressed in these cells. For this we used the primers: DYSF31-F (5′-GTGTGAACAGACCCACGAT-3′) and DYSF33-R (5′-GTCGTACAGCTCCACCACAA3′).

To sequence the complete *DYSF* cDNA, we used the PCRTiler v1.42 program[31] (http://pcrtiler.alaingervais.org:8080/PCRTiler/index.jsp) to design 17 primer sets to amplify ~500 bp cDNA segments that overlapped by ~50 bp and spanned the entire 6.9 kb *DYSF* cDNA (Table S1). cDNAs from cell cultures (corresponding to 40 ng input RNA) were amplified by PCR using Hotmaster Taq DNA polymerase (5 PRIME, Gaithersburg, MD, USA) as follows: 95°C for 5 min. 30 cycles of 95°C for 30 sec, 59.1°C for 30 sec, 72°C for 1 min, then 72°C for 10 min. PCR products were analyzed by gel electrophoresis and amplified products were purified and sequenced.

Similarly, primers were designed (Table S2) to amplify through and sequence *DYSF* intron 44i using 20 ng of genomic DNA from patient cells and blood samples using identical PCR conditions.

For RNA expression analyses, RNA was extracted and expression of normal and PE44.1 containing mutant RNA was evaluated by RT-PCR using primers that distinguish the two mRNA forms based on amplicon size (primers DYSF44/45-F and DYSF44/45-R [Table S3]). These primers span the exon 44–45 junction and generate a 143-bp amplicon from the normal cDNA (exon 44 + 45) and 320-bp amplicons from the mutant cDNA containing PE44.1 (exon 44 + PE44.1 + 45). Primers for beta-2-microglobulin (*B2M*, Bio-Rad) served as a RNA quality and loading control. cDNAs (corresponding to 20 ng input RNA) were amplified using Hotmaster Taq DNA polymerase as follows: 94°C for 2 min, 30 cycles of 94°C for 20 sec, 58°C for 20 sec, 65°C for 1 min, then 65°C for 10 min. PCR products were analyzed by gel electrophoresis.

For quantitative PCR (Q-PCR), cDNAs (corresponding to 20 ng input RNA) were amplified using primers that distinguish PE44.1-containing mutant RNA (DYSF 44.1-Q F and R) and normal RNA (DYSF 44/45-Q F.2 and R.2) (Table S3). Primers for *GAPDH* were used to normalize RNA levels. Primers specific to sequences spanning the junction of exons 50 and 51, present in all *DYSF* forms, were used to determine the total *DYSF* mRNA levels, and this served as the 100% *DYSF* expression value for each sample to approximate the relative expression of the mutant and normal exon 44/45 splice forms. For Q-PCR, we used DyNAmo HS SYBR Green qPCR Kit reagents (Thermo Scientific) and a Bio-Rad CFX384 C-1000 Touch Real-Time PCR Detection System. The PCR conditions were 95°C for 15 min, 45 cycles of 94°C for 10 sec, 58°C for 30 sec, 72°C for 30 sec, then 72°C for 10 min followed by melt curve analysis (65–95°C) to ensure product quality.

Allelic discrimination assays

TaqMan Probes were designed (Applied Biosystems) to distinguish normal and mutant alleles of the novel point mutation we identified in intron 44i of the two MM patients (Table S4). These were used in PCR reactions (Taqman Genotyping Master Mix Kit; Applied Biosystems) to amplify 10 ng of genomic DNA from the two MM patients, their immediate family members, 112 unrelated MM or LGMD2B patients (representing 81 pedigrees), and 724 DNA samples from a random population of normal individuals and those with unrelated diseases. PCR conditions were as follows: 95°C for 10 min. then 50 cycles of 92°C for 15 sec, 60°C for 1 min. PCR products were analyzed on a Bio-Rad CFX384 C-1000 Touch Real-Time PCR Detection System using the allelic discrimination software.

Monocyte assay for DYSF expression and serum CK expression

The relative level of DYSF protein expression was determined for patients P1 and P2, their relatives, and eight additional unrelated dysferlinopathy patients. The monocyte assay[25] and CK assay[32] used for this were performed as described previously.

AON transfections

The 44i mutation we identified leads to inclusion of an in-frame pseudoexon that disrupts the normal DYSF protein sequence. We hypothesize that inhibiting the splicing of PE44.1 would allow restored synthesis of normally spliced *DYSF* transcripts. We used Human Splicing Finder[33] and Rescue-exonic splicing enhancer (ESE)[34] online tools to design three AONs targeting potential ESE sequences within PE44.1 that could enhance its inclusion in spliced mRNA, along with a nonspecific scrambled AON that does not target this region (Table S5). These AONs were synthesized as 2′-O-methyl RNA with full-length phosphorothioate backbones (Integrated DNA Technologies, Coralville, IA, USA). iFDM cells from patient P1, P2, and normal NHDF-2 fibroblasts were allowed to differentiate for indicated lengths of time to form myotubes. Cells were transfected with each AON (600 nmol/L) (or TE buffer or medium only ("0 Added") as control) using Oligofectamine (Life Technologies) and the manufacturer's protocol. After the indicated times, RNA was extracted and the expression of normal and PE44.1 containing mutant RNA was evaluated by RT-PCR or quantitative RT-PCR.

Statistics

Statistical significance was evaluated using one-way analysis of variance (ANOVA) with post-hoc Tukey tests. For this we used Prism 5.0 statistical analysis software (GraphPad Software, San Diego, CA, USA).

Results

Identification of a deep intronic mutation in *DYSF* intron 44

The two index MM patients in our study, P1 and P2, do not express detectable DYSF protein in either their muscles or monocytes. Exon sequencing determined that they are heterozygous for a nonsense mutation in *DYSF* exon

32 (c.3444_3445delTGinsAA) that causes a premature stop codon within the C2D domain. Further sequencing analyses of *DYSF* exonic regions failed to identify a second pathogenic mutation on the other allele, suggesting that this mutation lies within noncoding regions of the gene. To identify the mutation on the other allele, we first established a myogenic cell culture system with cells from the patients and normal controls. Skeletal muscle cells or tissue were unavailable for our studies. We therefore generated myogenic cell lines from dermal fibroblasts cultured from patient skin biopsies. The fibroblasts from patients, along with normal control fibroblasts, were converted to iFDM cell cultures using lentiviral constructs to introduce a tamoxifen-inducible form of the myogenic regulator MyoD, which drives the myogenic program. In addition, lines were immortalized by introducing hTERT to extend their proliferative lifespan. Upon treatment of cells with tamoxifen, cultures contained numerous multinucleate myotubes and expressed differentiated muscle proteins such as myosin heavy chain as shown in Figure 1A, and on very rare occasion were observed to spontaneously contract. These lines thus provide an unrestricted supply of patient-derived myogenic cells with a high capacity to differentiate.

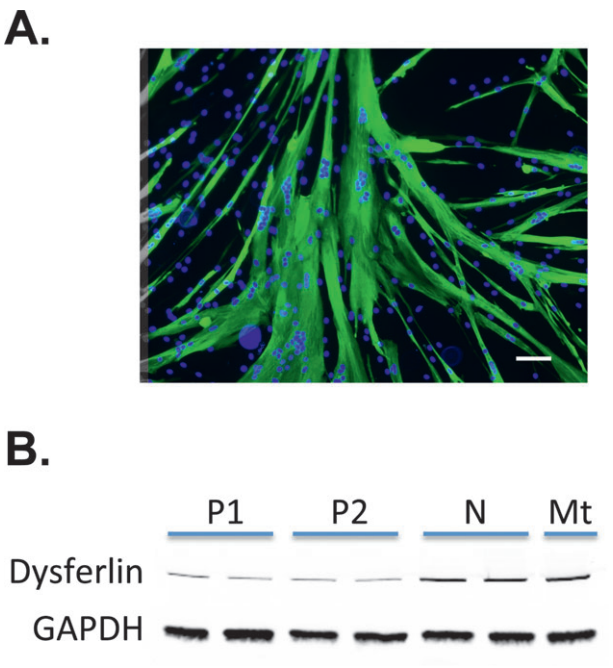

Figure 1. (A) Myosin heavy chain (MHC) expression in differentiated iFDMs derived from patient P1 dermal fibroblasts. Cells induced with TMX were cultured in DM for 9 days then stained with anti-MHC antibody (green). Nuclei are stained blue. Numerous multinucleate myotubes form, making these cultures very useful for myogenic studies. (Scale bar 100 μm). (B) Western blots show dysferlin protein in iFDMs from patients P1 and P2, normal fibroblasts (N) cultured in DM for 8 days, and human UBic myotubes (Mt) in DM for 7 days. iFDMs from patients express lower levels of DYSF than normal iFDMs, and this appears to be of normal size. GAPDH levels are shown as a control for protein loading (10 μg protein/lane). iFDMs, inducible fibroblast-derived myogenic cell; DM, differentiation medium.

Western blots containing protein from differentiated patient-derived iFDMs probed with C-terminal anti-DYSF antibodies (NCL-Hamlet) showed low levels of DYSF protein of apparently normal size (at ~20–40% the amount in normal iFDMs) (Fig. 1B). Similar results were obtained with anti-N-terminal DYSF antibody (not shown). Therefore, although DYSF protein was not detected in muscles or monocytes from these patients, low levels of DYSF protein are produced in these mutant cell cultures. The known mutation in these patients causes a premature stop codon within exon 32. Accordingly, one anticipates that this should result in a mutant transcript that should, in turn, generate a truncated protein (~130 kDa); we did not observe such a truncated protein, presumably because nonsense-mediated decay eliminates this mutant transcript. We therefore surmised that the DYSF protein of apparently normal size detected in vitro must have been derived from the allele without an exonic mutation.

To explore this further, we prepared cDNA using RNA from differentiated iFDM cells from derived patients P1, P2, and normal control NHDF-2 fibroblasts. We first used PCR primers that amplify the cDNA region around the known exon 32 mutation to determine whether transcripts carrying this mutation are expressed in the patient-derived iFDMs. Sequence analysis of amplified RT-PCR products showed that RNA did not contain the c.3444_3445delTGinsAA exon 32 nonsense mutation but rather contained only the wild-type (TG) sequence in this region, indicating that the *DYSF* mRNAs are produced only from the allele without this exonic mutation. This finding was consistent with the possibility that the mRNA products of the exon 32 mutant allele are likely degraded via rapid nonsense-mediated mRNA decay mechanisms. To further define the structure of the mRNA produced in the mutant iFDMs, PCR primer sets that generate 17 overlapping amplicons (Table S1) were used to sequence the full 6.9-kb *DYSF* cDNA from these cells, including 341 bp of 5′UTR and 246 bp of 3′UTR sequence. Most of these primer sets generated amplicons of the same size when comparing cDNAs from patients P1, P2, and normal differentiated iFDM cells (Fig. 2A, panels A and D). However, two of the overlapping primer sets revealed a novel amplification product only in the patient cDNAs (Fig. 2A, panels B and C, arrows). These two primer pairs span the junction of *DYSF* exons 44 and 45 (reference: *DYSF* mRNA variant 8, the predominant isoform in skeletal muscle). Using additional PCR primers that flank this 44/45 junction, we amplified cDNAs from skeletal muscle biopsy tissue RNA from Patient 1 and an unrelated, nonsymptomatic

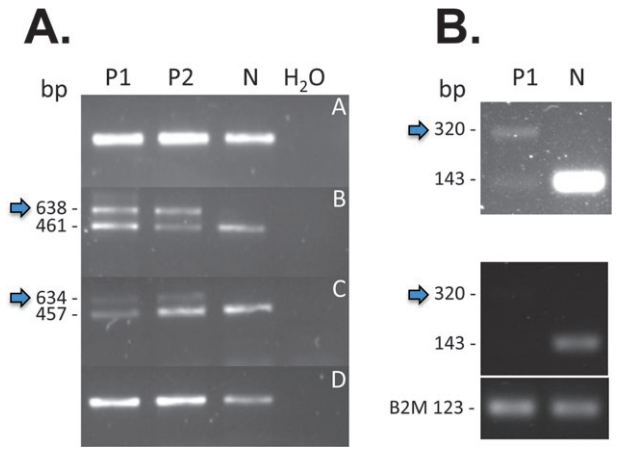

Figure 2. Identification of the *DYSF* intron 44i mutation. (A) RT-PCR of differentiated iFDM cDNA from two patients (P1, P2) shows novel amplicons (arrows) in patient samples using two primer sets (13F+R and 14F+R) (panels B and C) but not with any other sets (e.g., 9F+R and 15F+R) (panels A and D), indicating the presence of additional sequence within the patient cDNA in this region. Each PCR product was sequenced to identify the inserted sequence. (B) RT-PCR of cDNA from skeletal muscle tissue from patient P1 shows very low-level expression of *DYSF* mRNA compared to muscle from a normal control individual (N), and this includes mutant and wild-type transcripts for this locus. Primers that flank the exon 44/45 junction were used to distinguish mutant (320 bp) and normal (143 bp) cDNAs (also see Fig. 7). The top panel is a brighter gel exposure than the bottom panels, allowing visualization of the PCR products in patient muscle. Lower two panels show the same exposure for both the *DYSF* and *B2M* loading control PCR products (123 bp). *DYSF*, dysferlin; iFDM, inducible fibroblast-derived myogenic cell.

individual. As shown in Figure 2B, very low amounts of *DYSF* transcripts are present in the patient's muscle tissue and include both mutant and normal splice forms as detected by the two amplification products (320 and 143 bp, respectively). Only the normal cDNA amplification product is observed in the normal control muscle.

Subsequent sequence analysis of amplicons from each patient and control iFDM cell cDNA revealed that the novel amplicons contained 177 bp of intron 44i sequence spliced into the cDNA at the exon 44–exon 45 junction, maintaining the normal reading frame (Fig. 3). As a result, 59 amino acids are inserted into the protein sequence after amino acid 1629 (isoform 8). The patients therefore express a novel pseudoexon (PE), which we termed PE44.1, derived from sequences within *DYSF* 44i that are spliced into the mature transcript.

We sequenced the *DYSF* 44i region in genomic DNA from iFDMs and from blood samples from both patients and compared it with the genomic NCBI reference sequence. Sequence analysis revealed a point mutation in both patients nearly midway in intron 44i (c.4886+1249 (G>T) (Fig. 4A). This (G>T) mutation, which occurs 2 bp after the 3′ end of the PE44.1 insertion sequence, generates a consensus splice donor sequence at that site that promotes the aberrant splicing of PE44.1 into the mature transcript (Fig. 4B). Along with the novel splice donor site created by this (G>T) mutation, analysis of the intronic sequence upstream of PE44.1 reveals that other sequence elements required for splicing are also present in this region. As shown in Figure 4C, there is a conserved splice acceptor site at the 5′ end of PE44.1 along

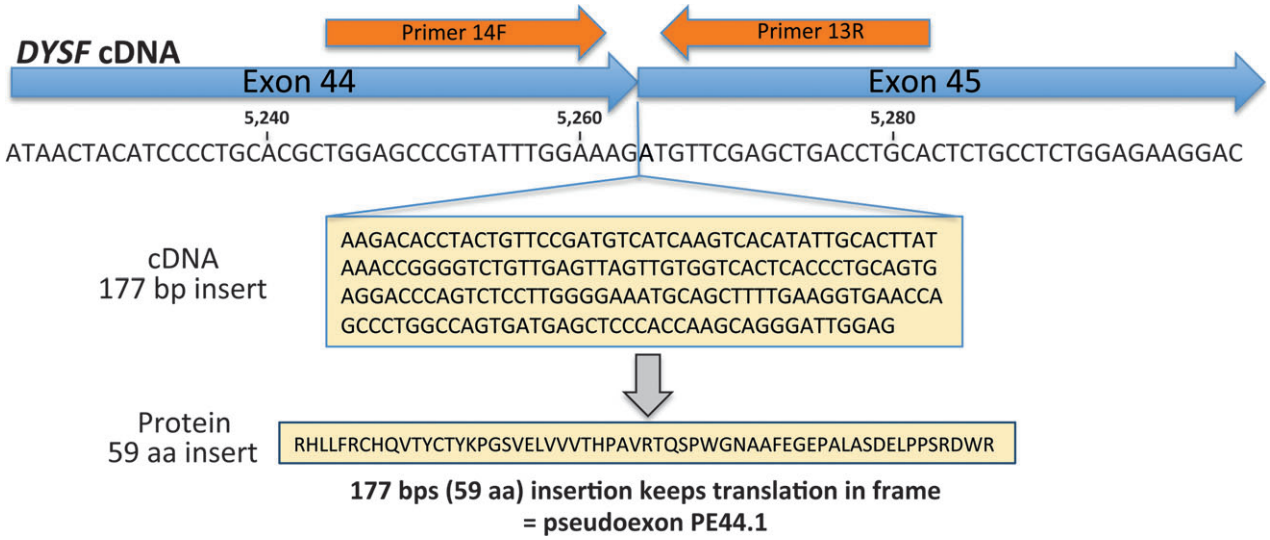

Figure 3. cDNA sequencing showed that patients P1 and P2 have an insertion of 177 nt at the junction of exons 44 and 45. This insertion maintains the reading frame and leads to inclusion of 59 additional amino acids in the protein sequence. The mRNA from these patients therefore contains a novel pseudoexon, PE44.1, spliced into the coding sequence.

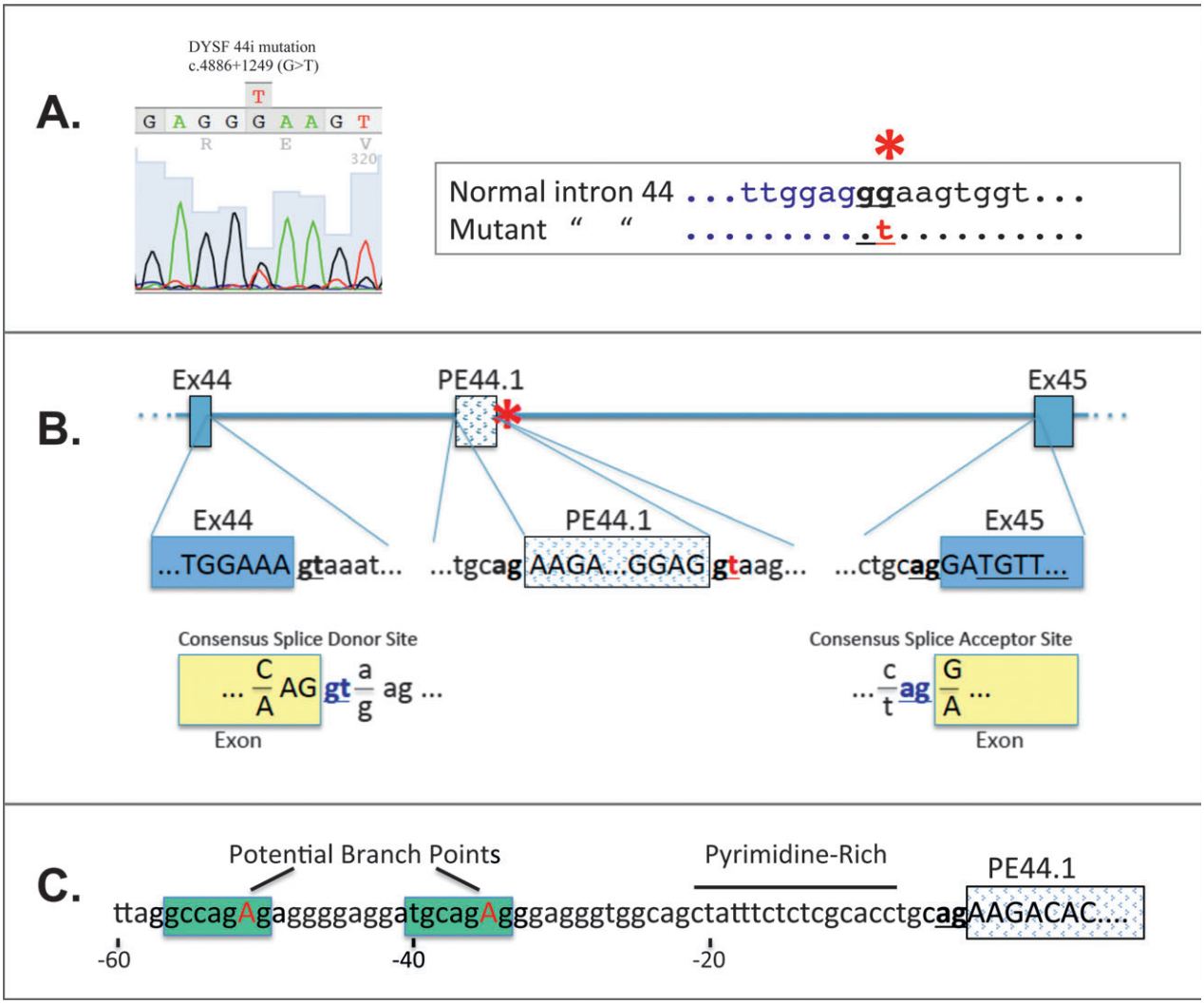

Figure 4. A novel deep intronic point mutation leads to inclusion of PE44.1 in the mature mRNA of patients P1 and P2. (A) Genomic sequencing of dysferlin (*DYSF*) intron 44i shows that patients are heterozygous for a point mutation (c.4886+1249 (G>T)). The location of this 44i mutation, indicated with an asterisk (*), creates a novel splice donor consensus sequence at the 3′ end of the PE44.1 sequence (B). (C) The intronic sequence upstream of PE44.1 contains additional consensus sites required for mRNA splicing including a splice acceptor site at the 5′ end of PE44.1, an adjacent pyrimidine-rich region and two potential lariat branch point consensus sequences that could be used to promote splicing. These sequences, in the presence of (c.4886+1249 (G>T)) mutation, allow the new pseudoexon PE44.1 to be spliced between exons 44 and 45.

with a required pyrimidine-rich region immediately upstream and two potential lariat branch point sequences (as identified by Human Splicing Finder version 2.4.1[33]), which is typically 20- to 50-bp upstream of the splice site. Therefore, multiple elements required by the splicing machinery are in place within this intronic region to allow the aberrant splicing of PE44.1 within the mRNA in the presence of this (G>T) point mutation.

In addition to the (c.4886+1249 (G>T)) mutation, complete sequence analysis of all the *DYSF* cDNA amplicons from patients P1 and P2 identified four other common sequence variants in their cDNA relative to the reference sequence (Table 1). Sequence analysis of their genomic DNA within *DYSF* intron 44i identified six additional polymorphisms (Table 2). All of these are common, previously identified polymorphisms that have not been found to cause disease.

The alternate *DYSF* splice forms present in patients P1 and P2 cells are shown in Figure 5A. Our cDNA amplification and sequencing results show that both normal and mutant PE44.1 mRNA splice forms are present in patient muscle and differentiated iFDM cells, typically in similar proportions (Figs. 2, 7, 9). The impact of PE44.1 inclusion in the *DYSF* mRNA and protein is further shown in

Table 1. cDNA sequence variants in Miyoshi myopathy patients P1 and P2.

SNP name	Ref.	Var.	Genotype 8597 (P1)	Genotype 8601 (P2)	Type	nt position	AA position	Exon	Sequence	Primers	Global MAF	Chromosomal location
rs2303596	T	C	C|C	C|C	Synonymous	c.1827T>C	p.(D609=)	20	ATGTGGATGA[T/C]GCCATCCAGT	6F+R	T = 0.4132/900	2:71780215
rs2288355	A	T	T|T	T|T	Synonymous	c.2583A>T	p.(S861=)	25	TTGGGCTCTC[A/T]GTGGATGAGA	8F+R	A = 0.4463/972	2:71795152
rs2303606	C	A	A|A	A|A	Synonymous	c.4008C>A	p.(I1336=)	38	GTGCTTAGAT[C/A]CTGGCATGGG	11F+R	A = 0.4784/1042	2:71838597
rs62145939	G	A	A|A	A|A	Synonymous	c.4731G>A	p.(E1577=)	43	GACCCCAGGA[G/A]TGCTTGGTCC	13F+R	A = 0.0101/21	2:71886100
–	TG	AA	TG|AA	TG|AA	Indel	c.3444_3445delTGinsAA	p.(Y1148X)	32	TTGGTGAAGA[T/A][G/A]GGAACCGCTA	10F+R		2:71817342-3

Reference (Ref.) and variant (Var.) alleles found in patients P1 and P2 and reported in the dbSNP database are shown. None of these SNP variants cause amino acid changes. The indel in exon 32 (c.3444_3445delTGinsAA) is a pathogenic mutation. The global minor allele frequency (MAF) and chromosomal location (GRCh37/hg19 assembly) are indicated, along with primer sets used to amplify and sequence these regions.

Table 2. Genomic DNA sequence variants in *DYSF* intron 44 of Miyoshi myopathy patients P1 and P2 and relatives.

SNP name	Ref.	Var.	8597 (P1)	8601 (P2)	8599	8600	8602	8603	nt position	Sequence	Primers	Global MAF	Chromosomal location
Novel	G	T	G|T	G|T	G|T	G|G	G|T	G|G	c.4886+1249G>T	GGATTGGAGG[G/T]AAGTGGTAGGT	i44.2F+R	Novel[1]	2:71889030
rs3791825	A	G	G|G	G|G	G|G	G|G	G|G	G|G	c.4886+1320A>G	CTGGCGCAGG[A/G]CCTCAGGCTA	i44.2F+R	A = 0.1387/301	2:71889101
rs3791826	C	G	G|G	G|G	G|G	G|G	G|G	G|G	c.4886+1375C>G	AGTGGGTGGG[C/G]GTGTGTCAGG	i44.2F+R	C = 0.1722/374	2:71889156
rs2303598	C	T	T|T	T|T	C|T	C|T	T|T	T|T	c.4887-162C>T	TACACACACA[C/T]TCAGGCCCAG	i44F+13R	C = 0.3747/816	2:71891236
rs2303599	C	T	T|T	T|T	T|T	T|T	T|T	C|T	c.4887-37C>T	TTGGGTGCCC[C/T]GTGTTGGCTG	i44F+13R	C = 0.2544/554	2:71891361
rs55689153	A	G	G|G	G|G	A|G	A|G	G|G	G|G	c.4887-1199A>G	TAGGGAAGGA[A/G]GGGCCCTGCC	i44.5F+R	A = 0.2929/637	2:71890199
rs3791827	C	G	G|G	G|G	C|G	C|G	G|G	G|G	c.4887-1083C>G	CTCATGTGCC[C/G]ACCACCGCTG	i44.5F+R	C = 0.4004/871	2:71890315

Genomic variations within *DYSF* intron 44 in patients P1, P2, and relatives are listed. The novel mutation c.4886+1249 (G>T) results in PE44.1 inclusion in mature mRNAs.
[1]The novel variant has not previously been described in the dbSNP database (http://www.ncbi.nlm.nih.gov/SNP/). Other variations are reported in the dbSNP database and have not been shown to be pathogenic. The primer sets used to amplify and sequence these regions are shown.

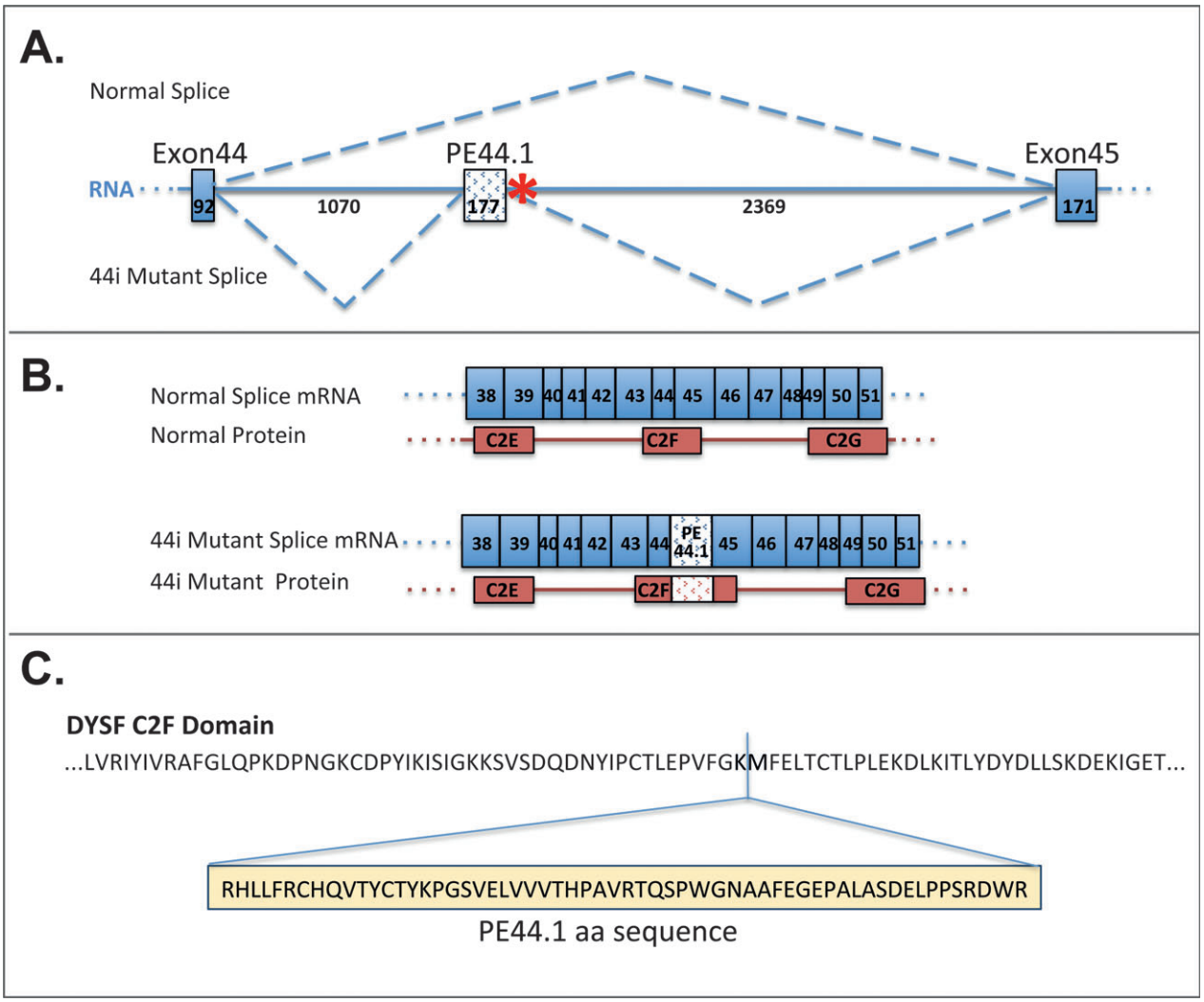

Figure 5. Normal and mutant PE44.1 mRNA are expressed through alternative splicing of the dysferlin (*DYSF*) transcripts. (A) The mRNA structure within the *DYSF* exon 44–intron 44i–exon 45 region is shown along with the normal and mutant splicing patterns. Numbers along the RNA indicate the size of each element in bp. The site of the 44i mutation (c.4886+1249 (G>T)) is indicated with an asterisk (*). (B and C) The normal and mutant splice products (including PE44.1) are shown (displaying the region of *DYSF* from exons 38–51). Also shown are the normal and mutant proteins. PE44.1 results in a 59 amino acids insertion within the normal C2F domain (normally 84 aa), creating a large disruption in this region.

Figure 5B and C. *DYSF* exons 44 and 45 encode part of the conserved C2F domain of DYSF. Insertion of the PE44.1 sequence leads to the in-frame insertion of 59 amino acids within the C2F domain, a large disruption that is likely to significantly impair protein function. This 59 amino acid sequence is unique and not homologous to any other peptide or protein structure.

Pedigree analysis

We amplified and sequenced genomic DNA from blood samples taken from immediate relatives of P1 and P2 to determine the inheritance of all sequence variants in *DYSF* 44i, as well as the *DYSF* exon 32 mutation previously identified in these patients. Figure 6 shows the *DYSF* genotypes of the family, revealing compound heterozygous inheritance of the *DYSF* 44i and exon 32 mutations in only the affected individuals P1 and P2, and the maternal inheritance of the *DYSF* 44i mutation responsible for PE44.1 expression. One other sibling is a non-symptomatic carrier of this mutation. DYSF protein expression in blood monocytes is absent or negligible in Patients 1 and 2 as expected from previous analyses of dysferlinopathy patients.[25] The segregation of all *DYSF* intron 44i allelic variants in the immediate family members is shown in Table 2.

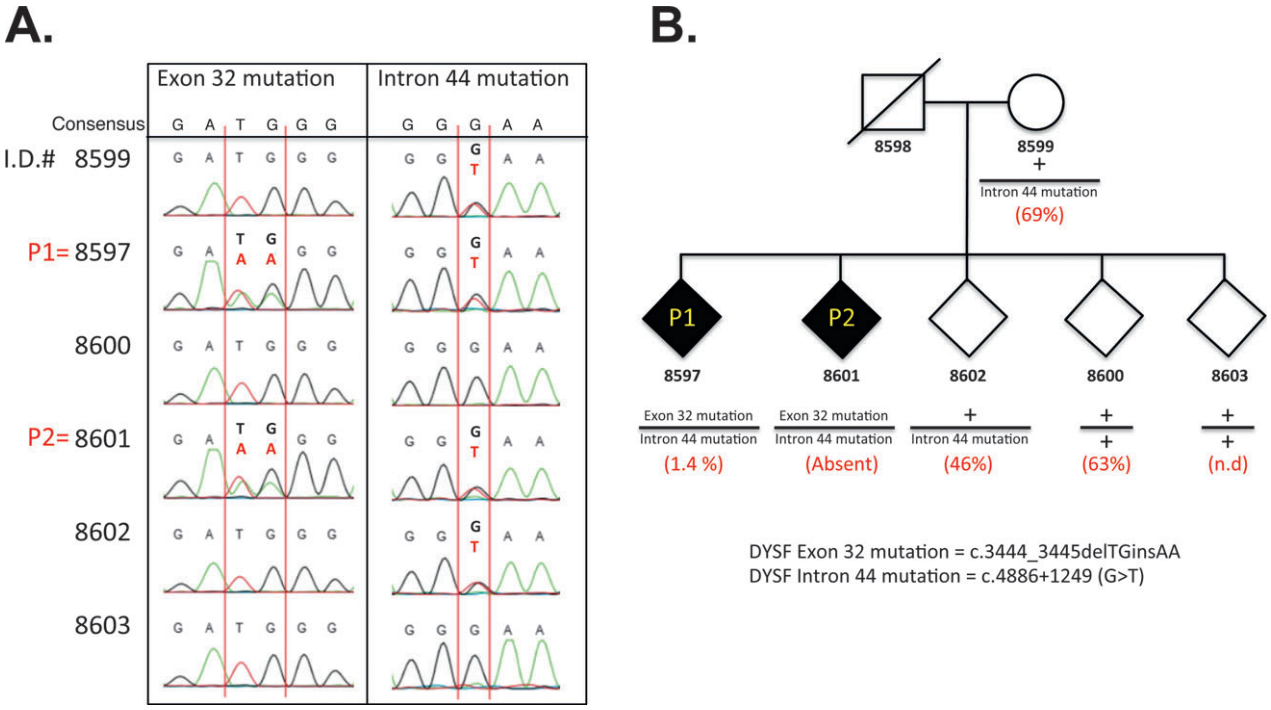

Figure 6. Analysis of genomic DNA from four immediate relatives of patients P1 and P2 reveals the inheritance pattern of the two mutations in this family. (A) Genomic DNA from each family member (listed by global I.D.) was amplified and sequenced using primers flanking the previously known dysferlin (*DYSF*) exon 32 mutation in these patients as well as the new *DYSF* 44i mutation associated with PE44.1 expression. Mutant nucleotides are shown in red. (B) Results show maternal inheritance of the *DYSF* 44i mutation. The expression of dysferlin protein in blood monocytes from each individual is shown in parentheses, with levels presented as the proportion of levels in normal control samples. (n.d., not done).

Table 3. Dysferlin allele variants and the relative dysferlin expression in eight patients that previously had only one or neither pathogenic *DYSF* allele identified by exome sequencing.

Patient No	Age of onset	CK levels	Allele 1	Allele 2	Dysferlin expression in monocyte assay[1]
JF01	28	3,369	c.1834C>T (p.Q612X)	c.4886+1249 G>T	Absent
JF14	3	300	–	–	Absent
JF15	18	198	c.3534C>T (p.I1178)	–	Absent
JF19	18	10,000	c.2997G>T (p.W999C)	–	Absent
JF32	17	2,800	–	–	9%
JF35	20	1,800	c.857T>A (p.V286E)	c.4886+1249 G>T	Absent
JF67	32	28,000	c.5341G>A (p.G1781R)	–	Absent
JF85	17	5,675	c.2997G>T (p.W999C)	–	10%

[1]The relative expression of dysferlin in monocytes is presented as the proportion of the level in normal control samples.

Prevalence of the deep intronic *DYSF* (c.4886+1249 (G>T)) mutation

We used an allelic discrimination assay to screen genomic DNA from 114 patients (81 pedigrees) clinically diagnosed with either MM or LGMD2B, along with 724 individuals from a random population (either normal or with an unrelated disease), using the patient P1, P2 and their four immediate family members as a reference. For this, TaqMan primers and probes were designed that distinguish the (c.4886+1249 (G>T)) point mutation from the normal genomic sequence in *DYSF* 44i. Using these assays, we found that only the two patients and two immediate family members carry this mutation.

In second phase of this study, we performed separate analyses of eight suspected dysferlinopathy patients that had only one or neither of their pathogenic *DYSF* mutations identified by exon sequencing. These patients were

screened for the c.4886+1249 (G>T) mutation by sequencing. As shown in Table 3, DYSF protein was low or absent in these patients, with serum CK, an indicator of muscle damage, elevated in most. Of the eight patients screened, two carried the c.4886+1249 (G>T) variant allele.

AON-mediated pseudoexon PE44.1 skipping

The inclusion of PE44.1 leads to a disruptive insertion within the DYSF protein. We therefore hypothesized that interventions that prevent the splicing of this pseudoexon into the mature mRNA should promote the synthesis of normal mRNA. We designed AONs directed against three possible exonic splice enhancer sequences within PE44.1 (Table S5, Fig. 7A). Blocking these enhancer sequences could reduce the amount of PE44.1 included in mature transcripts. These AONs were transfected into patient and normal control iFDM cells and mRNAs were analyzed 2–8 days later. As shown in Figure 7B, AON1 treatment for 2 days did not detectably affect the levels of the mutant or normal transcripts and was similar to controls treated with TE or a nontargeting scrambled AON. However, AON2 and AON3 reduced the relative levels of the mutant splice form containing PE44.1, and led to an increase in the levels of the normal mRNA splice form in cells from both patients P1 and P2 (Fig. 7B–D). For example, as shown in Figure 7C and D, the PE44.1 mutant form of RNA represented ~32–34% of the *DYSF* mRNA in P1 control cultures (TE or SCR scrambled control oligo), and ~41% in P2. AON2 treatment for 2 days reduced this mutant form to ~12% and 7% of the total *DYSF* levels in P1 and P2, respectively, while AON3 reduced it to ~15% and 6% (P1, P2, respectively). Concomitantly, there was an increase in the normal transcript levels in these cells: AON2 increased the normal form from ~45% of *DYSF* mRNA to ~70% in P1 cell, and from 38–44% to 78% in P2 cells. AON3 increased the normal form from ~45% of *DYSF* mRNA to ~66% in P1 cell, and from 38–44% to 92% in P2 cells. As expected, no PE44.1 containing mRNA was expressed in normal control cells. These results demonstrate that AONs can significantly modify mRNA splicing to inhibit mutant PE44.1 inclusion, which could potentially restore normal DYSF protein levels and function in these cells.

We found that treatment of patient iFDMs with AON3 can indeed induce the synthesis of DYSF protein as well as higher levels of normal *DYSF* transcripts that do not contain PE44.1 (Figs. 8 and 9). Here, TMX-induced iFDM cells were treated with AONs after 6 days of differentiation, at a point when cells are undergoing fusion to form myotubes in these cultures. Eight days after adding AON3, there was a significant increase in DYSF protein detectable by western blotting (Fig. 8A–C). Elevated protein levels were not detectable in AON3-treated cells after only one day of AON3 treatment (Fig. 8B and C), however, there was a dramatic effect at the RNA level, with reduced expression of the mutant PE44.1 form and increase in the normal splice form (Fig. 9A and B). After 3 days of AON3 treatment, DYSF protein levels were significantly higher in cells from both patients, while normal control cells showed no differences due to AON3. The elevated DYSF protein levels persisted through 8 days post-AON3 addition even though medium containing the AONs was removed on day 3. The effects of AON3 on the relative abundance of the PE44.1 and normal mRNA splice forms were also observed through 8 days post-AON3 addition (Fig. 9A and B). Therefore, AON-mediated skipping of PE44.1 can restore more normal levels of both *DYSF* mRNA and protein in these mutant cells.

Discussion

An ongoing concern in studies of the dysferlinopathies is that in ~17% of patients with this recessive disorder (described in Universal Mutation Database for Dysferlin (UMD-DYSF, v.1.1 26 April 2013, http://www.umd.be/DYSF/)[24]), only one disease-causing mutation is identified. Because most mutational studies involve exon analysis, the other alleles likely involve mutations outside exon regions. In a family in which two affected individuals had only one mutation identified by sequencing exonic regions, we directly sequenced cDNA representing the entire *DYSF* mRNA in the patients' myogenic cells, identifying an intronic sequence that was inserted within the cDNA. This insertion was generated by a novel point mutation deep within intron 44 (c.4886+1249 (G>T)), designated mutation 44i, which creates a new splice donor site consensus sequence and alters splicing of the *DYSF* mRNA to include a novel 177 nt pseudoexon (PE44.1) in the spliced mRNA. In addition to the index family in which we identified this mutation, subsequent screening of eight individuals, chosen because they had one or both pathogenic *DYSF* alleles unknown despite complete exon sequence analysis, revealed that two of the eight (25%) carried this c.4886+1249 (G>T) mutation. Therefore, this mutation might be relevant to a broader population of dysferlinopathy patients whose mutations have not been defined through routine exon sequencing.

Inclusion of PE44.1 within the mRNA leads to an insertion of 59 amino acids within the C2F domain of DYSF. This C2F domain appears to play an important role in DYSF dimerization and membrane localization.[10,11] Our protein analysis in myogenic cells in vitro detected low levels of DYSF protein of apparently normal size (~237 kDa) in iFDM cells from patients. The 59

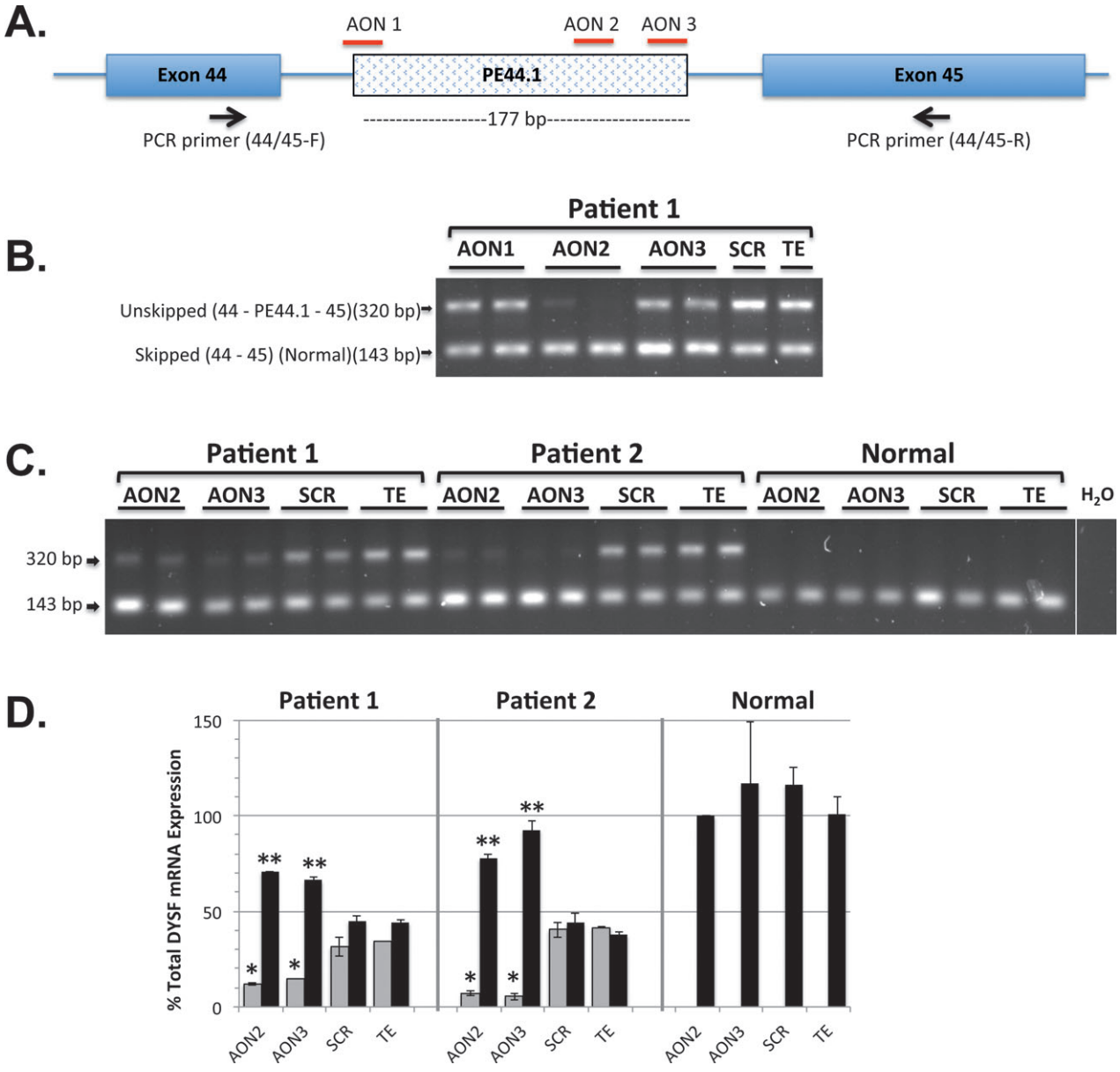

Figure 7. Antisense oligonucleotide-mediated skipping of PE44.1 in iFDM cells from patients P1 and P2. (A) AON1, AON2, and AON3 (see Table S5) target potential exonic splicing enhancers in PE44.1 in the areas shown. Primers within exon 44 and 45 were used to amplify cDNAs from iFDMs treated with AONs (duplicate cultures for each) to distinguish normal mRNA transcripts (143-bp product containing exon 44 + 45) from mutant PE44.1 transcripts (320 bp product containing exon 44 + PE44.1 + 45). (B) iFDM cells from Patient P1 treated with AON2 and AON3 (duplicate cultures for each) expressed reduced amounts of PE44.1 mutant mRNA and slightly higher normal *DYSF* mRNA compared with AON1-treated, nonspecific scrambled (SCR) AON-treated or TE-treated cells, which showed approximately equal proportions of mutant PE44.1 and normal mRNAs. TMX-induced iFDMs were in DM for 9 days then treated with AONs in DM for an additional 2 days. (C) A separate experiment using the same experimental conditions, patient P1, P2, and normal iFDMs (duplicate cultures for each treatment) showed that AON2 and AON3 treatments again reduced PE44.1 mutant mRNA expression and increased the relative abundance of normal *DYSF* mRNA. As expected, normal iFDMs only expressed normal *DYSF* transcripts. (D) Quantitative RT-PCR analysis of the same RNAs in (C) show that treatment if patient iFDMs with AON2 and AON3 significantly reduces the expression of the mutant transcripts (gray bars, mean ± SD, $*P < 0.05$) and increases expression of the normal transcripts (black bars, mean ± SD, $**P \ll 0.05$) compared to SCR and TE controls. The relative expression of each form is calculated using the amplification of a PCR product spanning the exon 50/51 junction as representative of 100% *DYSF* expression. iFDM, inducible fibroblast-derived myogenic cell; AON, antisense oligonucleotide; *DYSF*, dysferlin.

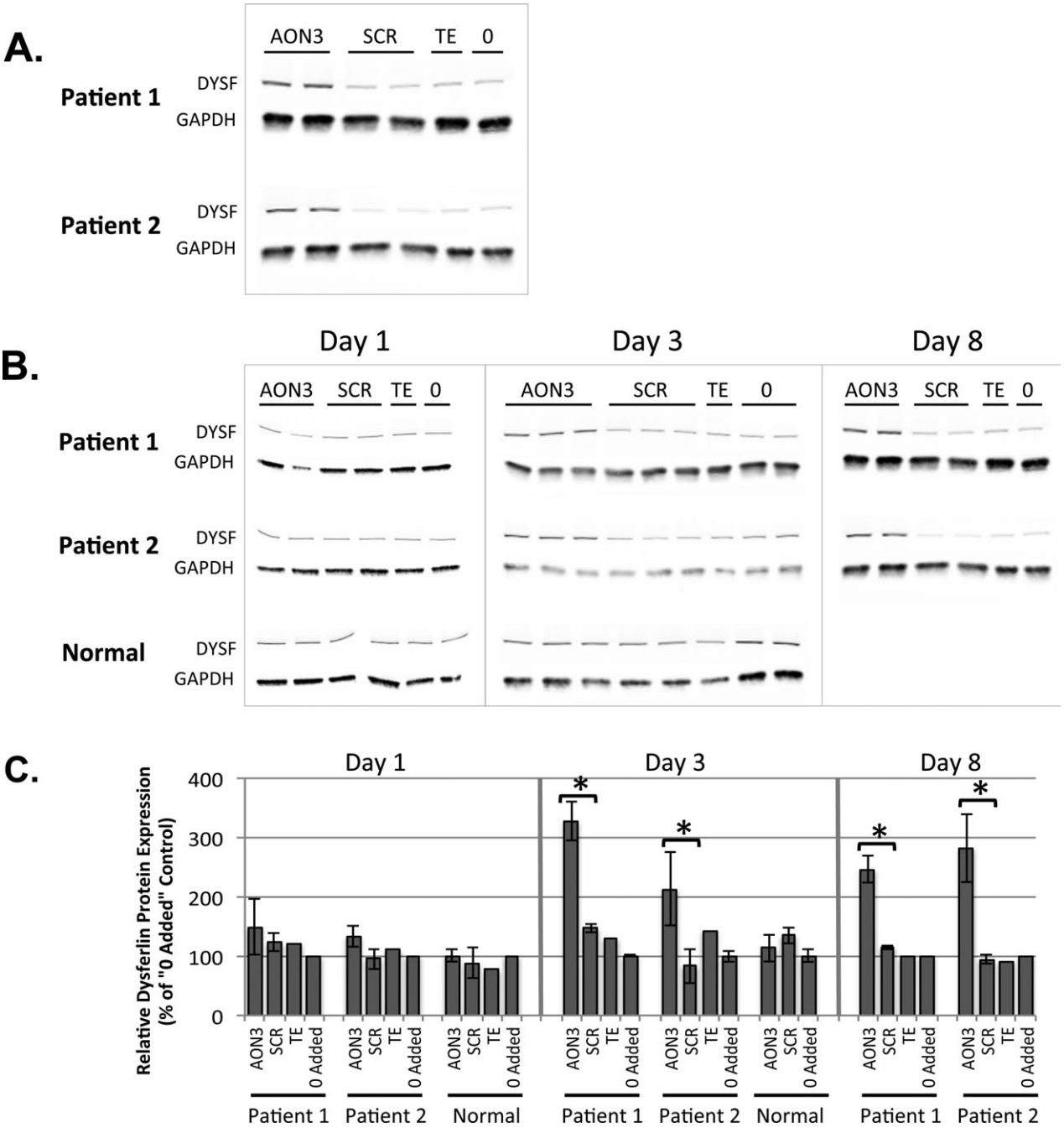

Figure 8. Treatment of patient iFDMs with AON3 directed to PE44.1 induces dysferlin protein expression. TMX-induced iFDMs (duplicate or triplicate cultures as shown) were cultured in DM for 6 days then treated with AONs in DM (or TE buffer or medium only [0] as controls). Cells were collected for protein analysis 1, 3, and 8 days after AON addition. For the 8-day samples, medium with AONs was removed on day 3 and replaced with DM only. (A) Western blots show that after 8 days of AON3 treatment there was a dramatic increase in DYSF protein expression compared with control cells. (B) DYSF protein levels were unchanged after 1 day but increased after 3 days of AON3 treatment. (The 8-day data are the same as in panel A, repeated for visual continuity). GAPDH expression served as a control for protein loading (5 μg protein/lane). (C) Quantitation of the bands shown in (A and B) reveals that there is a significant increase in DYSF protein in AON3-treated cultures compared with SCR oligo-treated controls (mean $\pm$ SD, $^*P < 0.05$). Protein levels in normal control iFDM cultures are not affected by AON treatments. iFDM, inducible fibroblast-derived myogenic cell; AON, antisense oligonucleotide; *DYSF*, dysferlin; DM, differentiation medium.

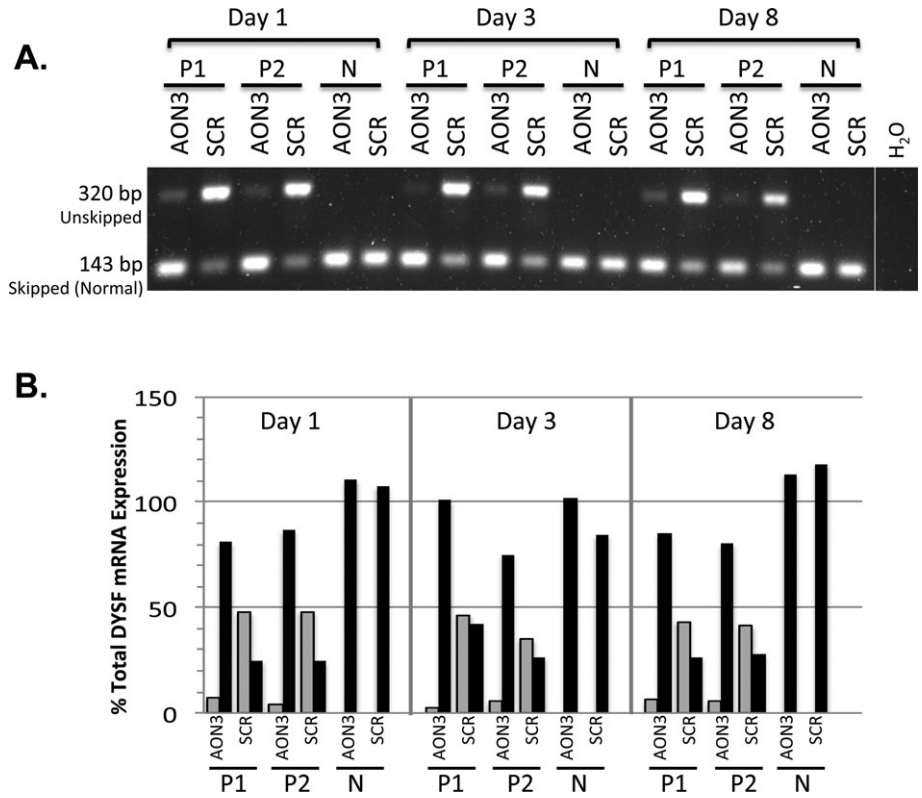

Figure 9. AON3 treatment of patient iFDMs alters expression of *DYSF* PE44.1 mutant and normal mRNA splice forms at 1, 3, and 8 days after AON addition. (A) RT-PCR analysis of mRNA from cultures collected in parallel with those in Figure 8 shows that treatment if Patient 1 (P1) and Patient 2 (P2) iFDMs with AON3 reduces the expression of the PE44.1 mutant transcript and increases normal transcript expression. Normal iFDMs (N) express only the normal *DYSF* form, not affected by AON treatments. (B) Quantitative RT-PCR analysis of the same mRNAs confirms the affects of AON3 treatment. (PE44.1 mutant transcript expression: gray bars; normal transcript expression: black bars). The relative expression of each form is calculated as shown in Figure 7D. AON, antisense oligonucleotide; iFDM, inducible fibroblast-derived myogenic cell; *DYSF*, dysferlin; PCR, polymerase chain reaction.

amino acids encoded by PE44.1 are predicted to add an additional 6.7 kDa to the full-length protein, a ~3% size difference (~244 kDa vs. ~237 kDa) that is likely to be indistinguishable on the standard SDS-PAGE gel system used. Therefore, in this in vitro experimental paradigm, we cannot be certain whether the low amount of DYSF protein observed is derived only from the residual normally spliced transcripts or from a combination of normal and mutant splice forms. It is conceivable that the mutant protein containing the additional 59 amino acids is unstable because of some combination of protein misfolding or aggregation, leading to its degradation.

The intron 44i (c.4886+1249 (G>T)) variant reported here is the first deep intronic pathogenic point mutation described in the *DYSF* gene. Mutations that involve the expression of pseudoexons have been identified in other genes associated with muscular dystrophy including dystrophin[35–37] and calpain 3.[38,39] However, in contrast with the present *DYSF* mutation, these generally lead to frameshifts and premature stop codons that prevent protein expression. Currently, 173 intronic variants have been identified within the *DYSF* gene (Leiden Muscular Dystrophy Pages v. DYSF130329, 29 March 2013, http://www.dmd.nl/nmdb/home.php?select_db=DYSF). In contrast with the deep intronic mutation reported here, ~75% of these 173 variants are near intron/exon boundaries or within ~70 bp of exons, regions more likely to be interrogated using routine mutation screening methods. Mutations in these exon-flanking regions could affect important branch point or other conserved sequences needed for splicing. Of those, ~42% are variants with no known pathogenicity. There are 45 currently known variants deeper within intronic sequences but ~82% of these, most of them single-nucleotide variants, have no known pathogenicity; those associated with disease involve larger deletions or insertions spanning exon/intron junctions.

Given that the 44i point mutation in our case leads to an aberrant inclusion of PE44.1, a clear therapeutic strategy to overcome the effects of this mutation is to use exon-skipping strategies to bypass the mutant pseudoex-

on. This approach is effective in modifying aberrant splicing of other pseudoexons[36,37,39,40] (reviewed[41,42]). AONs designed to block specific ESEs or other sequences required for splicing can be used to prevent the mRNA splicing machinery from including targeted exons (or pseudoexons) in the mature mRNA. This results in a truncated mRNA and, if no frameshifts occur as a result of the skip, the formation of truncated proteins that potentially retain partial function that is sufficient to improve overall cellular function. In the case presented here, the structure of the deep intronic 44i mutation and resulting PE44.1 aberrant splicing presents a unique and valuable opportunity to apply exon-skipping therapeutics to bypass DYSF pathogenic mutations. AONs designed to skip PE44.1 splicing will restore the normal mRNA splicing pattern and thus normal protein structure. This presents a "best-case scenario" for exon-skipping outcome if the skipping process is efficient and resulting protein synthesis is robust.

Our data show that AONs targeting PE44.1 sequences can indeed modify the splicing pattern of the mutant mRNA, reducing the aberrantly spliced form that includes PE44.1 and concomitantly increasing the normal mRNA form. This is followed temporally by a significant increase in DYSF protein levels. Additional studies are required to determine the nature of the AON-induced proteins, which appear to be of normal full length, but could also include the mutant form.

AON-mediated exon-skipping technologies are now in clinical trials for genetic diseases.[43–46] Encouraging pioneering work on the development of therapeutic exon-skipping reagents has come from Duchenne muscular dystrophy (DMD) cell and animal models showing that AON-mediated exon skipping is effective both in vitro and in vivo.[47–49] Clinical trials are underway using AONs to promote dystrophin exon 51-skipping, which could benefit ~13% of DMD patients (eteplirsen [AVI-4658], Sarepta Therapeutics and drisapersen [PRO051], Prosensa Therapeutics). AONs targeting other dystrophin mutations are under development as well. Results vary, but show encouraging improvements in dystrophin expression and muscle function in patients treated with AONs.[43–46,50]

Importantly for dysferlinopathies, there is evidence from a specific patient that exon skipping can improve diseased muscle function.[51] In that remarkable case, there was one severe *DYSF* mutant allele and one lariat branch point mutation upstream of exon 32. Approximately 10% normal DYSF protein levels were expressed because the branch point mutation caused exon 32 skipping, which maintained the reading frame and produced shorter but functional protein, resulting in mild symptoms. Experimentally, AON-mediated *DYSF* exon 32-skipping in cell cultures leads to the predicted shorter mRNA[52,53] and our unpublished observations. Analyses of *DYSF* exon/intron structure and DYSF protein domain structure suggest that patients with known mutations in a number of exons might derive some benefit from AON therapy.[53] This might include up to 20% of these dysferlinopathy patients. An additional 17% of patients have mutations yet to be fully defined, possibly including mutations within introns that could be targeted with AONs. Therefore, it is critical to determine the utility of AON-mediated skipping approach for the treatment of dysferlinopathies.

Our results provide compelling evidence that AON-mediated PE44.1-skipping could restore to clinically relevant levels of normal DYSF protein in patient's cells. Studies to demonstrate the functional effects of AON treatments on DYSF protein expression and function in cells from patients P1 and P2 are currently underway.

Acknowledgments

We thank M. C. Miceli and G. Kendall (UCLA School of Medicine) for advice with fibroblast immortalization and myogenic conversion methods, and J. Chen and C. Emerson, Jr. (U. Mass. Medical School) for the UBic cell lines used in this work. We thank the Cecil B. Day Foundation for supporting this work. R. H. B.'s laboratory also receives support from the NINDS (R01 FD004127-02, 5 R01 NS079836-03, 5 R01 NS065847-05, 1 R01 NS073873-03). P. C. S. is funded through the auspices of H. Robert Horvitz, an Investigator of the Howard Hughes Medical Institute (Massachusetts Institute of Technology). We also thank the Jain Foundation for providing support for M. H. and A. Ankala for his assistance with patient samples. We wish to acknowledge our gratitude for providing anonymized DNA samples for analysis from the following clinicians: A. Amato, C. Angelini, S. Appel, R. Barohn, S. Bohlega, D. Costigan, D. Cros, M. Cudkowicz, M. Dalakis, J. Doery, M. Fardeau, K. Felice, G. Fenichel, G. Ford, R. Griggs, A. Hahn, Y. Harati, F. Hentati, L. Hopkins, I. Illa, G. Karpati, M. King, N. Laing, E. Lichtenberg, I. Mahjneh, J. Mendell, G. Meola, R. Miller, G. Molderings, T. Munsat, G. O'Neill, M. Ross, L. Rowland, D. Sanders, R. Soffer, M. Sweet, Z. Simmons, A. Urtizberea, G. Wolfe, W. Wong.

Authorship

J. A. D and R. H. B. designed the study. O. U., P. C. S., B. R. R. N. and M. H. provided critical study design input. D. M. M.-Y. provided critical input on patient samples and study design. J. A. D., O. U., B. R. R. N. and M. H. acquired study data. J. A. D., O. U., P. C. S., B. R. R. N., M. H. and R. H. B. were responsible for data analysis and interpretation. J. A. D. and R. H. B. drafted the manuscript. All authors critically edited the content of the article and approved the final version.

Conflicts of Interest

J. A. D. and R. H. B. Jr. are employed by the University of Massachusetts Medical School and co-inventors on a patent application for antisense sequences and exon-skipping technology targeting dysferlinopathies. Dr. Brown reports grants from Cecil B. Day Foundation, grants from NIH- NINDS, other from Howard Hughes Medical Institute, during the conduct of the study; In addition, Dr. Brown has a patent "COMPOSITIONS AND METHODS FOR MODULATING DYSFERLIN EXPRESSION" pending. Dr. Dominov reports In addition, Dr. Dominov has a patent "COMPOSITIONS AND METHODS FOR MODULATING DYSFERLIN EXPRESSION" pending.

References

1. Lek A, Evesson FJ, Sutton RB, et al. Ferlins: regulators of vesicle fusion for auditory neurotransmission, receptor trafficking and membrane repair. Traffic 2012;13:185–194.
2. Posey AD Jr, Demonbreun A, McNally EM. Ferlin proteins in myoblast fusion and muscle growth. Curr Top Dev Biol 2011;96:203–230.
3. Liu J, Aoki M, Illa I, et al. Dysferlin, a novel skeletal muscle gene, is mutated in Miyoshi myopathy and limb girdle muscular dystrophy. Nat Genet 1998;20:31–36.
4. Bashir R, Britton S, Strachan T, et al. A gene related to *Caenorhabditis elegans* spermatogenesis factor fer-1 is mutated in limb-girdle muscular dystrophy type 2B. Nat Genet 1998;20:37–42.
5. Glover L, Brown RH Jr. Dysferlin in membrane trafficking and patch repair. Traffic 2007;8:785–794.
6. Hornsey MA, Laval SH, Barresi R, et al. Muscular dystrophy in dysferlin-deficient mouse models. Neuromuscul Disord 2013;23:377–387.
7. Laval SH, Bushby KM. Limb-girdle muscular dystrophies–from genetics to molecular pathology. Neuropathol Appl Neurobiol 2004;30:91–105.
8. Barthelemy F, Wein N, Krahn M, et al. Translational research and therapeutic perspectives in dysferlinopathies. Mol Med 2011;17:875–882.
9. Therrien C, Di Fulvio S, Pickles S, Sinnreich M. Characterization of lipid binding specificities of dysferlin C2 domains reveals novel interactions with phosphoinositides. Biochemistry 2009;48:2377–2384.
10. Xu L, Pallikkuth S, Hou Z, et al. Dysferlin forms a dimer mediated by the C2 domains and the transmembrane domain in vitro and in living cells. PLoS One 2011;6: e27884.
11. Azakir BA, Di Fulvio S, Salomon S, et al. Modular dispensability of dysferlin C2 domains reveals rational design for mini-dysferlin molecules. J Biol Chem 2012;287:27629–27636.
12. Marty NJ, Holman CL, Abdullah N, Johnson CP. The C2 domains of otoferlin, dysferlin, and myoferlin alter the packing of lipid bilayers. Biochemistry 2013;52:5585–5592.
13. Matsuda C, Hayashi YK, Ogawa M, et al. The sarcolemmal proteins dysferlin and caveolin-3 interact in skeletal muscle. Hum Mol Genet 2001;10:1761–1766.
14. Lennon NJ, Kho A, Bacskai BJ, et al. Dysferlin interacts with annexins A1 and A2 and mediates sarcolemmal wound-healing. J Biol Chem 2003;278:50466–50473.
15. Matsuda C, Kameyama K, Tagawa K, et al. Dysferlin interacts with affixin (beta-parvin) at the sarcolemma. J Neuropathol Exp Neurol 2005;64:334–340.
16. Huang Y, Verheesen P, Roussis A, et al. Protein studies in dysferlinopathy patients using llama-derived antibody fragments selected by phage display. Eur J Hum Genet 2005;13:721–730.
17. Cai C, Weisleder N, Ko JK, et al. Membrane repair defects in muscular dystrophy are linked to altered interaction between MG53, caveolin-3, and dysferlin. J Biol Chem 2009;284:15894–15902.
18. Huang Y, Laval SH, van Remoortere A, et al. AHNAK, a novel component of the dysferlin protein complex, redistributes to the cytoplasm with dysferlin during skeletal muscle regeneration. FASEB J 2007;21:732–742.
19. Han R, Campbell KP. Dysferlin and muscle membrane repair. Curr Opin Cell Biol 2007;19:409–416.
20. Klinge L, Laval S, Keers S, et al. From T-tubule to sarcolemma: damage-induced dysferlin translocation in early myogenesis. FASEB J 2007;21:1768–1776.
21. Klinge L, Harris J, Sewry C, et al. Dysferlin associates with the developing T-tubule system in rodent and human skeletal muscle. Muscle Nerve 2010;41:166–173.
22. Kerr JP, Ward CW, Bloch RJ. Dysferlin at transverse tubules regulates Ca homeostasis in skeletal muscle. Front Physiol 2014;5:89.
23. Pramono ZA, Tan CL, Seah IA, et al. Identification and characterisation of human dysferlin transcript variants: implications for dysferlin mutational screening and isoforms. Hum Genet 2009;125:413–420.
24. Blandin G, Beroud C, Labelle V, et al. UMD-DYSF, a novel locus specific database for the compilation and interactive analysis of mutations in the dysferlin gene. Hum Mutat 2012;33:E2317–E2331.
25. Ankala A, Nallamilli BR, Rufibach LE, et al. Diagnostic overview of blood-based dysferlin protein assay for dysferlinopathies. Muscle Nerve 2014;50:333–339.
26. Kimura E, Han JJ, Li S, et al. Cell-lineage regulated myogenesis for dystrophin replacement: a novel therapeutic approach for treatment of muscular dystrophy. Hum Mol Genet 2008;17:2507–2517.
27. Kendall GC, Mokhonova EI, Moran M, et al. Dantrolene enhances antisense-mediated exon skipping in human and

mouse models of Duchenne muscular dystrophy. Sci Transl Med 2012;4:164ra0.
28. Stadler G, Chen JC, Wagner K, et al. Establishment of clonal myogenic cell lines from severely affected dystrophic muscles – CDK4 maintains the myogenic population. Skelet Muscle 2011;1:12.
29. Wardrop KE, Dominov JA. Proinflammatory signals and the loss of lymphatic vessel hyaluronan receptor-1 (LYVE-1) in the early pathogenesis of laminin {alpha}2-deficient skeletal muscle. J Histochem Cytochem 2011;59:167–179.
30. Jeudy S, Wardrop KE, Alessi A, Dominov JA. Bcl-2 inhibits the innate immune response during early pathogenesis of murine congenital muscular dystrophy. PLoS One 2011;6:e22369.
31. Gervais AL, Marques M, Gaudreau L. PCRTiler: automated design of tiled and specific PCR primer pairs. Nucleic Acids Res 2010;38(Web Server issue):W308–W312.
32. Rosalki SB. An improved procedure for serum creatine phosphokinase determination. J Lab Clin Med 1967;69:696–705.
33. Desmet FO, Hamroun D, Lalande M, et al. Human Splicing Finder: an online bioinformatics tool to predict splicing signals. Nucleic Acids Res 2009;37:e67.
34. Fairbrother WG, Yeh RF, Sharp PA, Burge CB. Predictive identification of exonic splicing enhancers in human genes. Science 2002;297:1007–1013.
35. Ferlini A, Galie N, Merlini L, et al. A novel Alu-like element rearranged in the dystrophin gene causes a splicing mutation in a family with X-linked dilated cardiomyopathy. Am J Hum Genet 1998;63:436–446.
36. Gurvich OL, Tuohy TM, Howard MT, et al. DMD pseudoexon mutations: splicing efficiency, phenotype, and potential therapy. Ann Neurol 2008;63:81–89.
37. Khelifi MM, Ishmukhametova A, Khau Van Kien P, et al. Pure intronic rearrangements leading to aberrant pseudoexon inclusion in dystrophinopathy: a new class of mutations? Hum Mutat 2011;32:467–475.
38. Blazquez L, Azpitarte M, Saenz A, et al. Characterization of novel CAPN3 isoforms in white blood cells: an alternative approach for limb-girdle muscular dystrophy 2A diagnosis. Neurogenetics 2008;9:173–182.
39. Blazquez L, Aiastui A, Goicoechea M, et al. In vitro correction of a pseudoexon-generating deep intronic mutation in LGMD2A by antisense oligonucleotides and modified small nuclear RNAs. Hum Mutat 2013;34:1387–1395.
40. Rimessi P, Fabris M, Bovolenta M, et al. Antisense modulation of both exonic and intronic splicing motifs induces skipping of a DMD pseudo-exon responsible for x-linked dilated cardiomyopathy. Hum Gene Ther 2010;21:1137–1146.
41. Dhir A, Buratti E. Alternative splicing: role of pseudoexons in human disease and potential therapeutic strategies. FEBS J 2010;277:841–855.
42. Siva K, Covello G, Denti MA. Exon-skipping antisense oligonucleotides to correct missplicing in neurogenetic diseases. Nucleic Acid Ther 2014;24:69–86.
43. Cirak S, Arechavala-Gomeza V, Guglieri M, et al. Exon skipping and dystrophin restoration in patients with Duchenne muscular dystrophy after systemic phosphorodiamidate morpholino oligomer treatment: an open-label, phase 2, dose-escalation study. Lancet 2011;378:595–605.
44. Goemans NM, Tulinius M, van den Akker JT, et al. Systemic administration of PRO051 in Duchenne's muscular dystrophy. N Engl J Med 2011;364:1513–1522.
45. Kole R, Krainer AR, Altman S. RNA therapeutics: beyond RNA interference and antisense oligonucleotides. Nat Rev Drug Discov 2012;11:125–140.
46. Rodino-Klapac LR, Mendell JR, Sahenk Z. Update on the treatment of Duchenne muscular dystrophy. Curr Neurol Neurosci Rep 2013;13:332.
47. Mann CJ, Honeyman K, Cheng AJ, et al. Antisense-induced exon skipping and synthesis of dystrophin in the mdx mouse. Proc Natl Acad Sci USA 2001;98:42–47.
48. Aartsma-Rus A, Janson AA, Kaman WE, et al. Therapeutic antisense-induced exon skipping in cultured muscle cells from six different DMD patients. Hum Mol Genet 2003;12:907–914.
49. Alter J, Lou F, Rabinowitz A, et al. Systemic delivery of morpholino oligonucleotide restores dystrophin expression bodywide and improves dystrophic pathology. Nat Med 2006;12:175–177.
50. Mendell JR, Rodino-Klapac LR, Sahenk Z, et al. Eteplirsen for the treatment of Duchenne muscular dystrophy. Ann Neurol 2013;74:637–647.
51. Sinnreich M, Therrien C, Karpati G. Lariat branch point mutation in the dysferlin gene with mild limb-girdle muscular dystrophy. Neurology 2006;66:1114–1116.
52. Wein N, Avril A, Bartoli M, et al. Efficient bypass of mutations in dysferlin deficient patient cells by antisense-induced exon skipping. Hum Mutat 2010;31:136–142.
53. Aartsma-Rus A, Singh KH, Fokkema IF, et al. Therapeutic exon skipping for dysferlinopathies? Eur J Hum Genet 2010;18:889–894.

Supporting Information

Additional Supporting Information may be found in the online version of this article:

Table S1. Primers (forward [F] and reverse [R]) used to generate overlapping amplicons that span the entire dysferlin cDNA.

Table S2. Primers (forward [F] and reverse [R]) used to generate overlapping amplicons that span dysferlin intron 44.

Table S3. Primers (forward [F] and reverse [R]) used in RT-PCR assays to analyze RNA for expression for the dysferlin intron 44 mutant and normal transcripts.

Table S4. TaqMan primers (forward [F] and reverse [R]) and probes used in allelic discrimination assays to screen genomic DNA for the dysferlin intron 44 mutation.

Table S5. AONs targeting human exonic splicing enhancer sequences (ESE) in DYSF PE44.1. AONs for in vitro studies are 2′-*O*-methyl RNA with full-length phosphorothioate backbones.

